Ultrasonic Piezoceramic-polymer Composite Transducer
--- Dynamic Behavior and Effects of Heterogeneous Structure

Q. M. Zhang, X. Geng, Y. Shui, Wenwu Cao, and L. E. Cross
Materials Research Laboratory, The Penn State University
University Park, PA 16802

Abstract: A dynamic theory is developed for piezocomposites with 2-2 connectivity. By solving the coupled dynamic equations in the piezoceramic plate and polymer region subjected to the boundary conditions at the ceramic-polymer interface, the distributions of the elastic and electric variables in a composite are obtained. The electromechanical coupling factor, the acoustic impedance, the resonant frequency, and the elastic coupling between the polymer and ceramic at the thickness resonance can be determined. The effects of modes coupling on the thickness resonance and lateral resonance are elucidated and the dependence of the frequency of these resonant modes on the composite thickness can be estimated. Theoretical results are compared with experimental observations.

I. Introduction

The heart of an ultrasonic transducer is the piezoelectric element which performs the energy conversion between the electric form and mechanical form. To meet the broadened applicational needs and increase the signal sensitivity and resolution of an ultrasonic transducer, there is a constant effort on improving the piezoelectric transducer materials. The introduction of the piezoceramic polymer composites in the late seventies opened a new avenue of high quality ultrasonic transducer materials. The low insertion loss, short ringing time, adjustable acoustic impedance, as well as agility in the material properties are some of the advantages that a piezocomposite possesses.[1-4]

The typical configurations of the currently commercially available piezocomposites are either in 2-2 connectivity form or 1-3 connectivity form, as schematically drawn in figure 1. The important parameters for an ultrasonic transducer material are the electromechanical coupling factor, acoustic impedance, electric impedance, and mechanical quality factor, etc. In addition, unlike a monolithic piezoelectric material, the polymer phase in a composite is often piezoelectric inactive while it provides a low acoustic impedance path for the mechanical energy flow with the medium. Therefore, it is critical to have an effective elastic coupling between the polymer matrix and the piezoceramic elements so that the advantages of the low acoustic impedance of the polymer matrix and high electromechanical coupling factor of the ceramic elements can be fully made use of.

Being a diphasic material, the composite properties can vary over a wide range and most notably, as have been observed by many experiments, the properties of a piezocomposite will vary as the sample thickness is changed.[3] The periodic structure in a composite will also introduce resonant modes which may interfere with the thickness resonance and degrade the performance of the transducer.[5] To design an ultrasonic composite transducer properly and make best use of a composite material for a specific application require a quantitative understanding of how each design parameter affect the effective properties of a composite. It is the purpose of this paper to present the results of a recent theoretical modeling on establishing a quantitative structure-property relationship for the ultrasonic piezoceramic polymer composite as well as related experimental work. Due to the space limitation, only the results for the 2-2 composite will be presented.

II. Theory

For a typical 2-2 composite as shown in figure 1, the dimensions in the x_1- and x_2-directions can be taken as infinite; therefore, the problem is two-dimensional with no dependence on the x_2-component. For the results discussed here, the dimension in the x_3-direction (thickness t = 2L) is also assumed to be much larger than the lateral period d and the effect of the two end faces is neglected. The effect of the finite thickness and hence, the two end surfaces on the properties of a composite can be treated based on the results here with a proper summation of partial waves. They will be discussed

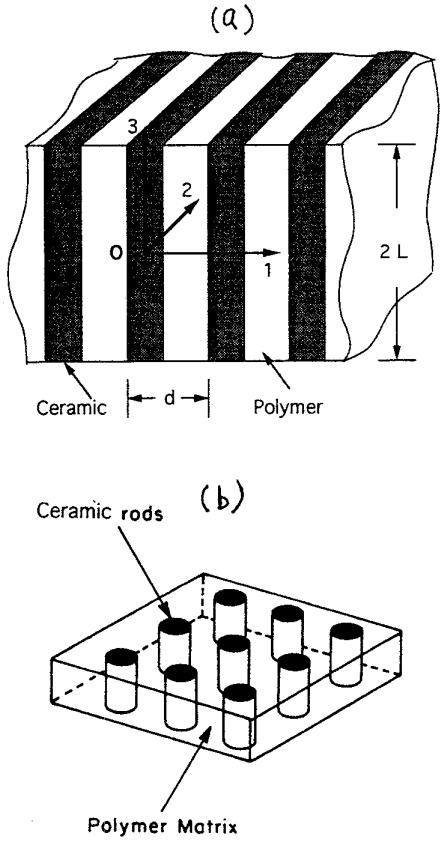

Figure 1. Schematical drawing of piezoceramic polymer composites with (a) 2-2 connectivity; (b) 1-3 connectivity.

in the future. The approach adopted here is similar to that used in treating the static properties of a piezo-composite.[6] That is, the elastic and electric equations for both the piezoceramic plate and polymer matrix are solved first, and the coupling between the two phases is established through the boundary conditions. Using the coordinate system in figure 1, the governing equations for the problem are

$$\frac{\partial T_3}{\partial x_3}+\frac{\partial T_5}{\partial x_1}=\rho\frac{\partial^2 u_3}{\partial t^2},\quad \frac{\partial T_1}{\partial x_1}+\frac{\partial T_5}{\partial x_3}=\rho\frac{\partial^2 u_1}{\partial t^2},\quad \text{and div}\,\vec{D}=0 \qquad (1)$$

where T_i are the stress tensors, $\vec{D}$ is the electric displacement, u_i are the elastic displacements and in eq. (1) and in the following the contracted notations for the stress and strain tensors are used. The constitutive equations for the piezoceramic phase are

$$\begin{aligned} T_1&=c^c_{11}u_{1,1}+c^c_{13}u_{3,3}-e_{13}E_3\\ T_3&=c^c_{13}u_{1,1}+c^c_{33}u_{3,3}-e_{33}E_3\\ D_1&=\varepsilon_{11}E_1+e_{15}(u_{3,1}+u_{1,3})\\ D_3&=\varepsilon_{33}E_3+e_{33}u_{3,3}+e_{11}u_{1,1} \end{aligned} \qquad (2)$$

where $u_{i,j}$ denote the derivative of u_i with respect to the jth-coordinate and E_i are the electric fields, c_{ij}^c are the elastic stiffness coefficients at constant E field, e_{ij} are the piezoelectric coefficients, ε_{ij} are the dielectric constants at constant strain, and D_i are the electric displacement vector. Similar equations can be written for the polymer phase with $e_{ij} = 0$ and all the other parameters replaced by

CH3416-5 0-7803-1847-1/95/$4.00©1995IEEE

those of the polymer. In the normal ultrasonic transducer operation frequency range, the quasi-electrostatic approximation can be used for the electric field,[7] i.e.

$$\vec{E} = -\nabla\Phi \qquad (3)$$

where Φ is the electric potential. Combining eqs (1), (2) and (3) yields the equation of motion for u_1, u_3, and Φ. For a harmonic motion, the general solution to the equation is of the form

$$u_3 = A \exp(i(hx_1 + \beta x_3 - \omega t))$$
$$u_1 = B \exp(i(hx_1 + \beta x_3 - \omega t)) \qquad (4)$$
$$\Phi = C \exp(i(hx_1 + \beta x_3 - \omega t))$$

where A, B, and C are three constants, ω is the angular velocity. Substituting equation (4) into eq. (1) through the constitutive relations, we obtain three homogeneous equations with three undetermined constants, A, B, and C. The condition for a non-trivial solution is that the determinant of the coefficients vanishes. For the ceramic plate, this implies

$$\begin{vmatrix} c_{33}^c\beta^2+c_{44}^c h^2-\rho\omega^2 & (c_{13}^c+c_{44}^c)\beta h & e_{33}\beta^2+e_{15}h^2 \\ (c_{13}^c+c_{44}^c)\beta h & c_{11}^c h^2+c_{44}^c\beta^2-\rho\omega^2 & (e_{15}+e_{31})\beta h \\ e_{33}\beta^2+e_{15}h^2 & (e_{15}+e_{31})\beta h & -(\varepsilon_{11}h^2+\varepsilon_{33}\beta^2) \end{vmatrix} = 0 \qquad (5)$$

Equation (5) yields three roots of h, denoted as h_1^c, h_2^c, and h_3^c, for each pair of ω and β, corresponding to the quasi-longitudinal, quasi-share, and quasi-electromechanical waves, respectively.

For each h_i^c, the ratio among A, B, and C can be determined and the general solutions have the form

$$u_3^c = \sum_i R_i^c f_i \cos(h_i^c x_1) \sin(\beta x_3)$$
$$u_1^c = \sum_i R_i^c g_i \cos(h_i^c x_1) \sin(\beta x_3) \qquad (6)$$
$$\Phi^c = \sum_i R_i^c t_i \cos(h_i^c x_1) \sin(\beta x_3)$$

where i in the summation runs from 1 to 3. f_i, g_i and t_i are the cofactors $A_{k1}(i)$, $A_{k2}(i)$, and $A_{k3}(i)$ of the determinant (5) (where h is replaced by h_1, h_2, and h_3 for i = 1, 2, and 3, respectively). In deriving equation (6), the symmetry conditions in both the x_1- and x_3-directions for a piezo-active mode have been used. Similar equations can be written for the polymer region except x_1 in equation (6) should be replaced by $(x_1 - d/2)$ and all the parameters used should be those of the polymer phase.

Eq. (6) and the corresponding equation for the polymer phase contain six constants, R_i^c and R_i^p (i = 1,2,and 3). They can be determined from the boundary conditions at the ceramic-polymer interface ($x_1 = \nu d/2$, where ν is the volume content of the ceramic in a composite), which are:

$$u_1^c = u_1^p,\ u_3^c = u_3^p,\ T_1^c = T_1^p,\ \text{and } T_5^c = T_5^p \qquad (7)$$

and

$$\Phi^c = \Phi^p \text{ and } D_1^c = D_1^p \qquad (8)$$

For six homogeneous equations with six undetermined constants (R_i^c and R_i^p), the condition for a non-trivial solution is that the determinant of the coefficients vanishes, i.e.,

$$R = |\text{ coefficients of } R_i\ | = 0 \qquad (9)$$

Eq. (9) is a transcendental equation which yields the relations between ω and β, the dispersion curves for the composite. From that, one can find R_i^c and R_i^p, and hence the various stress, strain, and electric field distributions in a composite at the resonant mode.

III. Results and Discussions

Shown in figure 2(a) is the dispersion curves for the two lowest branches of the dispersion curves calculated from eq. (9) for a 2-2 composite made of PZT-5H and Spurrs epoxy. The ratio ω/β at small βd from the branch 1 yields the effective velocity of the composite at constant D, v^D, in the x_3-direction. In figure 2(b), v^D as a function of the ceramic volume content is presented. For comparison, the experimental data measured from the corresponding composites as well as the result from an earlier quasi-static model (modified for 2-2 piezocomposites), which has been widely used,[4] are also shown. The agreement between the current theory and experiment is excellent. From the relations $\bar{\rho} = \nu\rho^c + (1-\nu)\rho^p$ and $\bar{Z} = \bar{\rho}\, v^D$, where ρ is the density, the acoustic impedance can be evaluated and the result for a 2-2 composite with PZT 5H ceramic plate and Spurrs epoxy is shown in figure 2(c).

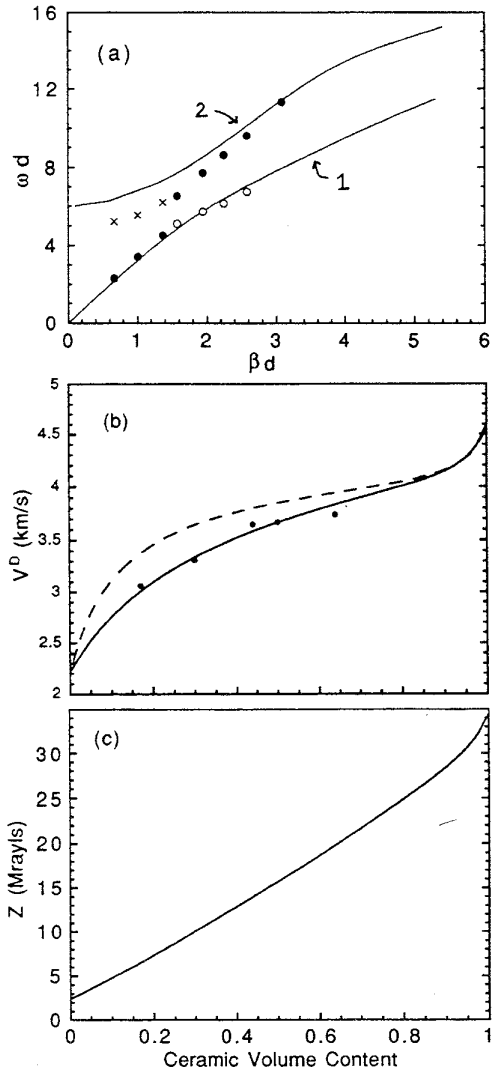

Figure 2. (a) The dispersion cerves for a 2-2 composite made of PZT 5H plates and Spurrs epoxy. Under the approximation that λ=2t, where t is the thickness of the composite, the experimentally observed resonant modes can be compared with the theoretical prediction.
(b) V^D as a function of the ceramic volume content for a composite made of PZT 5H and Spurrs epoxy.
(c) The acoustic impedance Z as a function of the ceramic volume content for a 2-2 composite with PZT 5H and Spurrs epoxy.

The information on the strain, stress, and electric field distributions in a composite at a resonant mode derived enables us to evaluate the electromechanical coupling factor for that resonance from the relation

$$k^2 = U_{int} / (U_E U_M) \qquad (10)$$

where U_{int}, U_E, and U_M are the exchange energy, electric energy, and mechanical energy terms in the total energy of a piezo-material, respectively,

$$U_{int} = \frac{1}{2} e_{ki}E_k S_i,\quad U_M = \frac{1}{2} s_{ij}^E S_i S_j,\quad U_E = \frac{1}{2} \varepsilon_{ij}^s E_i E_j \qquad (11)$$

For a composite material, the quantities in eq. (11) shoule be integrated on one repeating unit of the composite.

On the other hand, making use of the IEEE definition,[8]

$$\left(\frac{v^E}{v^D}\right)^2 = (1 - k_t^2) \qquad (12)$$

where v^E is the velocity at the constant E field, k_t can be calculated in a much simpler manner.

For a single phase material, v^E ($= \sqrt{c_{33}^E/\rho}$) can be found from the dispersion curve by setting E = constant in the wave equations. For a composite material discussed here, we assume that a similar approach can also be used in the limit of $\beta \rightarrow 0$ where the electric fields in the polymer and ceramic regions are nearly equal. Therefore, similar to the procedure of deriving v^D but utilizing only the elastic equations and boundary conditions, v^E for a composite can be obtained. The coupling factor k_t thus determined is plotted in figure 3, along with the experimental data from the corresponding composites and the result from the earlier quasi-static model (for 2-2 composites made of PZT 5H and Spurrs Epoxy). Good agreement is obtained between the theoretical prediction and the experimental data.

From the theoretical model developed, the dependence of k_t on the elastic properties of the polymer phase and the piezoelectric properties of the ceramic phase can be evaluated.

At the thickness resonance, the thickness t of a sample is equal to half of the resonant wavelength λ. Making use of this relation, the variation of the material properties of a composite with thickness ($\beta = 2\pi/\lambda = \pi/t$) can be extrapolated from the dispersion curves. With this spirit, the experimental results of the change of the resonant frequency for the thickness mode and the first lateral mode with the sample thickness are plotted in figure 2(a). The experimental data points can be described by the theoretical dispersion curves reasonably well even though the model here is initially intended to treat a composite of small βd.

Several observations can be made from figure 2(a). As a composite becomes thinner (βd increases), the thickness resonant mode approaches the lateral resonant mode, and as a result of modes coupling, the resonant frequencies for the two modes are affected. For a composite transducer, the thickness resonance is always marked in the impedance curve by the strongest resonant peak and having the largest ratio of $(f_p - f_s)/f_p$ where f_s and f_p are the series and parallel resonant frequencies. On the other hand, by nature, the lateral resonance, originated from the periodic structure of a composite, is weak and can be identified by the fact that u_3 at the center (u_3(cent)) of polymer region is 180° out of phase with that at the center of the ceramic plate. Based on these, on figure 2(a), the data points are marked by black dots for the thickness resonance and crosses for the lateral resonant modes. Above the modes coupling region, the resonant mode on the branch 1 gradually disappears. However, even though the frequency of the resonance in this region is close to or even higher than those marked by the crosses, u_3 in the polymer region and ceramic region are still in phase with a larger difference in the vibration amplitude between the two regions. The mode here is a result of the modes coupling and when the thickness mode moves away, the mode in this region disappears. Therefore, we do not mark them as either lateral or thickness resonance.

For all these resonant modes, the vibration amplitude of u_3 in the polymer region is always larger than that in the ceramic plate. It is also observed both experimentally and theoretically that for the thickness resonance on the branch 2 (above the modes coupling region), u_3 in the center of the polymer region is 180° out of phase with that in the center of the ceramic plate. In another words, u_3 in the polymer region and in the ceramic plate are in phase for the resonant modes on the branch 1 and out of phase for the resonant modes on the branch 2. Due to the fact that u_3 of the ceramic and polymer in the branch 2 is out of phase, the influence of the two end faces of a composite (traction free boundary condition when there is no acoustic load on a composite) will be more important. The model presented does not take this into account and hence, it is expected that the discripancy between the theory and experiment will become severe in the branch 2, as shown in figure 2(a).

An effective stress transfer between the polymer and ceramic plate requires u_3 in the two regions in phase and having nearly the same amplitude. Shown in figure 4 is the ratio of u_3(cent) of the polymer to u_3(cent) of the ceramic plate measured on the surface of a 2-2 composite with 44% ceramic content and d/λ=0.13, where the thickness resonant frequency f_t (at 770 kHz) is about half of the lateral resonant frequency f_l. The amplitude ratio between the two regions is equal to one up to a frequency of about 800 kHz, beyond that frequency, the vibration amplitude in the polymer phase increases rapidly. The phase between the vibrations in the two regions also exhibits the similar trend. The two vibrations are in phase up to about 950 kHz and above that, the two vibrations show large phase difference. This clearly sets a limit on the ratio of d/λ, beyond which the stress transfer between the two regions in a composite will be reduced significantly and the performance of a composite, hence, will be affected.

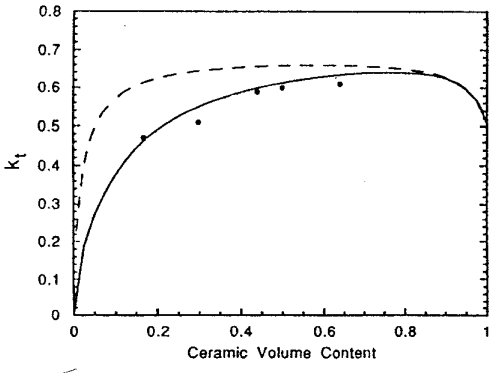

Figure 3. The thickness coupling factor as a function of the ceramic volume content for a 2-2 composite of PZT 5H piezoceramic and Spurrs epoxy.

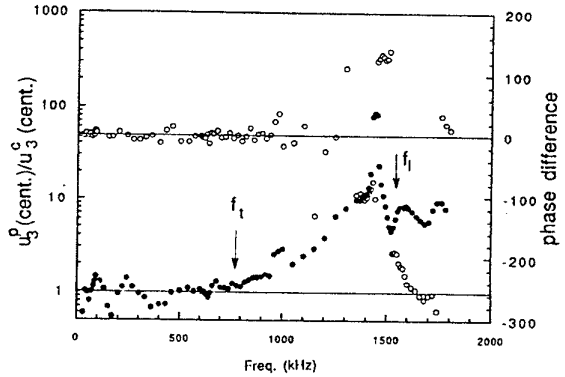

Figure 4. The ratio of the vibration amplitude of u_3 at the center of polymer gap (u_3^P) to that at the center of ceramic plate (solid circles) and phase difference between the two (open circles) measured at the surface of a 2-2 composite with ceramic volume content 44 %. The data was acquired using a laser dilatometer while the composite was driven by an electric field.

IV. Summary and Acknowledgement

In summary, a dynamic model on piezoceramic polymer composites is developed which provides near exact solution for a 2-2 piezocomposite at small d/t ratio. Based on this model, a quantitative relationship between the composite effective properties and the design parameters of constitunents is established, and the effect of the modes coupling between the thickness and lateral resonances on their resonant behavior (i.e. resonance frequency, strain and stress distributions, etc.) is elucidated. Extension of this model to 1-3 composite and to include the boundary conditions at the two end faces is currently underway.

The authors wish to thank Dr. J. Yuan and Dr. H. Kunkel for many stimulating discussions and for measuring the elastic properties of Spurrs epoxy. This work was supported by the Office of Navy Research under Grant No: N00014-93-1-0340.

References:

1. W. A. Smith and A. A. Shaulov, Ferro. 87, 309 (1988).
2. R. E. Newnham, et. al. Mater. in Engin. 2, 93 (1980).
3. T. R. Gururaja, et. al. IEEE Trans. on Sonics and Ultrasonics, SU 32, 499 (1985).
4. W. A. Smith and B. Auld, IEEE Trans. UFFC 38, 40 (1988).
5. B. A. Auld, et al., Proc. Ultrasonic Symp. (IEEE, 1983), p. 554.
6. Q. M. Zhang, et al., IEEE Trans. UFFC 41, (1994).
7. B. A. Auld, "Acoustic Fields and Waves in Solid" (John Wiley & Sons, New York, 1973).
8. IEEE Standard on piezoelectricity (ANSI/IEEE Standard 176-1987,1988).